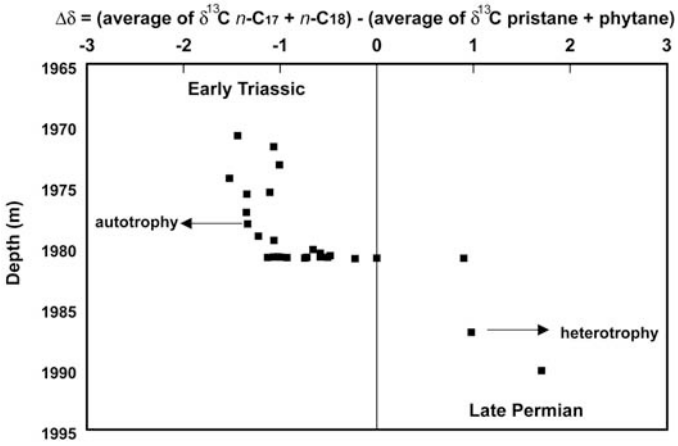

Fig. 4. $\Delta\delta$ = (average $\delta^{13}C$ of n-C_{17} and n-C_{18}) – (average $\delta^{13}C$ of pristane and phytane) ‰ (relative to VPDB standard in ‰) with depth (meters). Measurements determined by isotope-ratio-monitoring gas chromatography–mass spectrometry (IsoPrime, Micromass, Manchester, UK) of saturate, branched/cyclic, and n-alkane fractions [see (*14*) for 5A molecular sieving and compound-specific isotope analyses].

Australia, and must have been very localized. Because PZE also occurred in the contemporaneous seas off South China, localized high algal productivity probably played a key role in the formation of a petroleum-rich source rock in the Perth Basin.

References and Notes

1. D. Erwin, *Nature* **367**, 231 (1994).
2. M. J. Benton, R. J. Twitchett, *Trends Ecol. Evol.* **18**, 358 (2003).
3. P. B. Wignall, R. J. Twitchett, *Science* **272**, 1155 (1996).
4. Y. Isozaki, *Science* **276**, 235 (1997).
5. P. B. Wignall, A. Hallam, *Palaeogeogr. Palaeoclimatol. Palaeoecol.* **93**, 21 (1992).
6. A. H. Knoll, R. K. Bambach, D. E. Canfield, J. P. Grotzinger, *Science* **273**, 452 (1996).
7. L. R. Kump, A. Pavlov, M. Arthur, Y. Kato, A. Riccardi, *Abstracts of GSA Annual Meeting,* Paper 81-6 (Geological Society of America, Seattle, WA, 2–5 November 2003).
8. T. Trull *et al.*, *EOS Trans. Am. Geophys. Union* **82**, 306 (2001).
9. K. Grice *et al.*, *Geochim. Cosmochim. Acta* **60**, 3913 (1996).
10. R. E. Summons, T. G. Powell, *Geochim. Cosmochim. Acta* **51**, 557 (1987).
11. M. Koopmans *et al.*, *Geochim. Cosmochim. Acta* **60**, 4467 (1996).
12. K. Grice, P. Schaeffer, L. Schwark, J. R. Maxwell, *Org. Geochem.* **25**, 131 (1996).
13. Materials and methods are available as supporting material on *Science* Online.
14. B. M. Thomas *et al.*, *Aust. J. Earth Sci.* **51**, 423 (2004).
15. Sedimentary porphyrins provide a link to precursor chlorophylls in photosynthetic organisms indicative of primary production in paleowaters. Ni/VO porphyrin ratios are indicators of redox conditions (*30*).
16. $Fe_{HR} = Fe_D + Fe_P$ to Fe_T is an indicator of water-column redox conditions in ancient/modern environments (*17*, *31*). $Fe_{HR}/Fe_T > 0.4$ are typical for euxinic settings with pyrite formation in the water column. Fe_{HR}/Fe_T values < 0.4 are found in sediments below oxic bottom waters, where pyrite precipitates in the sediment. Fe_{HR}/Fe_T ratios < 0.4 do not exclude deposition in a euxinic environment but may indicate changes in the source/depositional setting (*17*).
17. T. F. Anderson, R. Raiswell, *Am. J. Sci.* **304**, 203 (2004).
18. D. E. Canfield, A. Teske, *Nature* **382**, 127 (1996).
19. R. J. Newton, E. L. Pevitt, P. B. Wignall, S. H. Bottrell, *Earth Planet. Sci. Lett.* **218**, 331 (2004).
20. C. Korte *et al.*, *Int. J. Earth Sci.* **93**, 565 (2004).
21. H. F. Passier *et al.*, *Nature* **397**, 146 (1999).
22. Y. Kajiwara, S. Yamakita, K. Ishida, H. Ishiga, A. Imia, *Palaeogeogr. Palaeoclimatol. Palaeoecol.* **111**, 367 (1994).
23. C. B. Foster, G. A. Logan, R. E. Summons, J. D. Gorter, D. S. Edwards, *Aust. Pet. Prod. Explor. Assoc. J.* **37**, 472 (1997).
24. K. Grice *et al.*, unpublished data.
25. J. M. Hayes, *Rev. Mineral. Geochem.* **43**, 225 (2001).
26. S. Schouten *et al.*, *Geochim. Cosmochim. Acta* **62**, 1397 (1998).
27. G. A. Logan, J. M. Hayes, G. B. Hieshima, R. E. Summons, *Nature* **376**, 53 (1995).
28. V. Schwab, J. E. Spangenburg, *Appl. Geochem.* **19**, 55 (2004).
29. R. D. Pancost *et al.*, *J. Geol. Soc. London* **161**, 353 (2004).
30. M. D. Lewan, J. B. Maynard, *Geochim. Cosmochim. Acta* **46**, 2547 (1982).
31. Y. Shen, A. H. Knoll, M. R. Walter, *Nature* **423**, 632 (2003).

32. We thank Origin Energy for collecting a unique, core-based maturity profile of the Hovea core of the Perth Basin. We also thank S. Wang, G. Chidlow, and Geoscience Australia (Canberra) for technical input and M. Kuypers, D. Fike, and two anonymous reviewers for comments. K.G. acknowledges the Australian Research Council for funding. C.Q.C. and Y.G.J. were supported by the China Ministry of Science and Technology and the National Natural Science Foundation of China. M.E.B. acknowledges Max-Planck-Gesellschaft for support. Work at the Massachusetts Institute of Technology was supported by NASA Exobiology grant NAG5-1236.

Supporting Online Material

www.sciencemag.org/cgi/content/full/1104323/DC1
Materials and Methods
Figs. S1 and S2
References

20 August 2004; accepted 6 January 2005
Published online 20 January 2005;
10.1126/science.1104323
Include this information when citing this paper.

Abrupt and Gradual Extinction Among Late Permian Land Vertebrates in the Karoo Basin, South Africa

Peter D. Ward,[1]* Jennifer Botha,[3] Roger Buick,[2] Michiel O. De Kock,[5] Douglas H. Erwin,[6] Geoffrey H. Garrison,[2] Joseph L. Kirschvink,[4] Roger Smith[3]

The Karoo basin of South Africa exposes a succession of Upper Permian to Lower Triassic terrestrial strata containing abundant terrestrial vertebrate fossils. Paleomagnetic/magnetostratigraphic and carbon-isotope data allow sections to be correlated across the basin. With this stratigraphy, the vertebrate fossil data show a gradual extinction in the Upper Permian punctuated by an enhanced extinction pulse at the Permian-Triassic boundary interval, particularly among the dicynodont therapsids, coinciding with negative carbon-isotope anomalies.

The Permian extinction is universally portrayed as the most catastrophic of all Phanerozoic mass extinctions (*1*), yet its cause remains problematic. Various hypotheses include climate change due to increased atmospheric CO_2 and/or CH_4 (*2*), the effects of extraterrestrial impact (*3*–*5*), the effects of the eruption of the Siberian Traps, and some synergistic combination of these (*6*), among others. An important test of any mechanism is a consideration of the pattern of extinctions. The marine extinctions are well described in several areas, notably Meishan, China (*7*). Here, we report new chemostratigraphic, biostratigraphic, and magnetostratigraphic data from multiple stratigraphic sections located in the Karoo basin of South Africa that provide an exceptionally detailed record of the terrestrial extinctions.

Permian-Triassic (P-T) strata in the central Karoo basin provide the most intensively investigated record of vertebrate fossils from

[1]Department of Biology, [2]Department of Earth and Space Sciences, University of Washington, Seattle, WA 98195, USA. [3]Karoo Paleontology, Iziko: South African Museum, Cape Town, South Africa. [4]Division of Geological and Planetary Sciences, California Institute of Technology, Pasadena, CA 91125, USA. [5]Department of Geology, Rand Afrikaans University, Johannesburg, South Africa. [6]Department of Paleobiology, MRC-121 Smithsonian Institution, Washington, DC 20013, USA.

*To whom correspondence should be addressed. E-mail: argo@u.washington.edu

the Upper Permian through the Triassic (*8*). These strata are dominantly fluvial overbank sediments deposited near the center of a subsiding retroarc foreland basin (*9*). We have sampled across 200 m of the Palingkloof Member of the Balfour Formation and the overlying Katberg Formation, where we recognize four units spanning the Upper Permian and Lower Triassic (*10*). Fossils were collected from these strata at five different areas. Hence, correlating the sections, which is difficult between fluvial sections and has been notably problematic in the Karoo (*11*), is critical.

To correlate the stratigraphy, we obtained a magnetostratigraphic record (Fig. 1) (*12*) from three sections [some data are also in (*13*)]. Samples from Unit II and Unit III are all of normal polarity (Chron N1), and we identified a reversed polarity magnetozone (R1) ~5 m beneath the Unit I-II contact (*14*). At Lootsberg and Wapadsberg, the normal-polarity zone extends well up into the Katberg Formation (Unit IV). At Lootsberg, where the youngest strata were sampled of all the sections, there is a change to reversed polarity (R2) above about 130 m and a final switch back to normal (N2) at the top. Given paleontological constraints (*8*), we correlate the long normal found in Units II, III, and most of IV with magnetozone SN1 of the classic German Trias sections (*15*) and thus define the top and bottom of the Griesbachian stage in the Karoo. The superjacent reversal at Lootsberg Pass is most parsimoniously correlated with magnetozone SR1 of central Germany, R2 of the Southern Alps, and GR1 of the Canadian Arctic. Although there is some uncertainty about the reversal pattern near the P-T boundary (*16*), recent records in Europe suggest that the boundary occurs just above the base of a reversed-to-normal-polarity transition in Germany, although there has been a recent report placing it slightly lower, in the uppermost part of the reversed chron (*17*). The base of Unit II is thus approximately coincident with the P-T boundary.

These correlations were tested by measuring sedimentary carbon isotope ($\delta^{13}C_{carb}$ and $\delta^{13}C_{org}$) stratigraphy at all the sections at meter or submeter sampling frequency (*12*) (Fig. 2), a finer resolution than has been done before (*18*). This earlier P-T isotope study in the Karoo found a single negative $\delta^{13}C_{carb}$ excursion approximately coincident with the last occurrence of the latest Permian

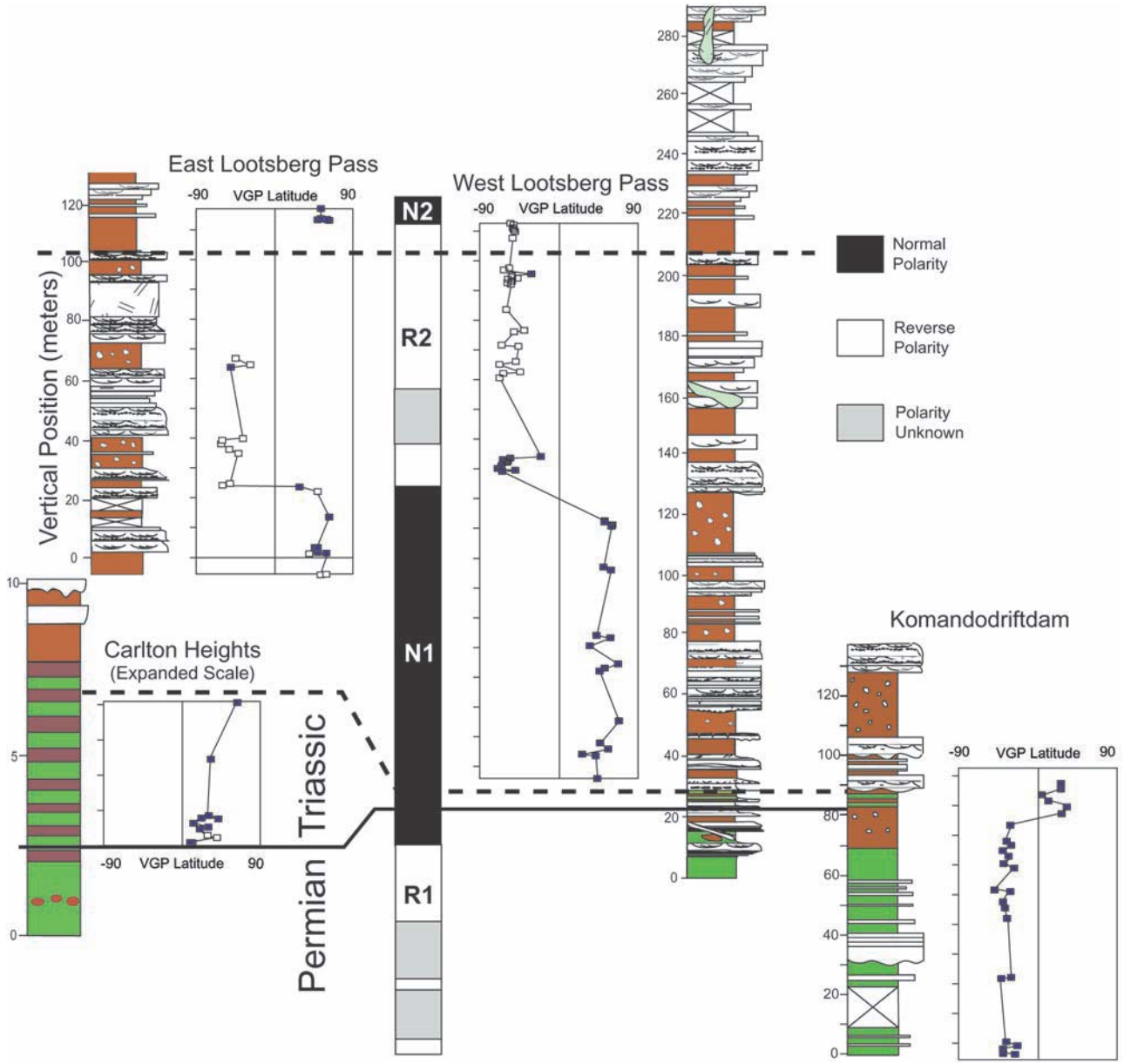

Fig. 1. Magnetostratigraphic correlation across the Karoo basin. The dashed lines represent the correlated positions between the stratigraphic sections.

zonal index fossil *Dicynodon*. The global $\delta^{13}C$ record for the P-T boundary period is known in varying detail from several dozen marine and fewer nonmarine sites (e.g., *19, 20*). Intensively sampled sections show a gradual decline in the sedimentary ^{13}C:^{12}C ratio upward through the Upper Permian, then a sudden decline of >2‰ at or near the paleontologically defined extinction boundary, followed by a gradual increase in $\delta^{13}C$. The sudden $\delta^{13}C$ decline precedes the formal P-T boundary based on the first occurrence of the Triassic conodont *Hindeodus parvus* at the global stratotype section and point (GSSP) P-T stratotype in Meishan, China, where the boundary has been placed at Bed 27. At Meishan, the lowest $\delta^{13}C$ values are found in Bed 25 (*7*), coincident with the level of maximal species disappearance (94% loss of then-extant marine invertebrates). Thus, the mass extinction and sharp negative excursion in $\delta^{13}C$ are slightly older than the formal stratigraphic boundary.

We sampled both bulk sediment and carbonate paleosol nodules for carbon isotope stratigraphy from our measured sections. Soil carbonate $\delta^{13}C$ ($\delta^{13}C_{carb}$) is a function of both the $\delta^{13}C$ of atmospheric CO_2 ($\delta^{13}C_{CO2}$) and the partial pressure of CO_2 in the atmosphere (pCO_2), and thus soil $\delta^{13}C_{carb}$ records can be more scattered than marine $\delta^{13}C_{carb}$ records (*21*). Nevertheless, the $\delta^{13}C_{carb}$ results show a prominent drop within Unit I that is consistent with our assessment that Unit I/Unit II contact marks the P-T extinction (Fig. 2). The $\delta^{13}C_{carb}$ values maintain a broad minimum in Unit II, a pattern similar to global marine $\delta^{13}C_{carb}$ records. The lowermost negative excursion in $\delta^{13}C_{carb}$ observed in the Karoo most parsimoniously correlates with the singular, lower Griesbachian negative $\delta^{13}C_{carb}$ excursion reported recently from a Late Permian–Late Triassic carbonate platform in the Nanpanjiang Basin, Guizhou Province, China (*22*). Furthermore, the broad swings in $\delta^{13}C_{carb}$ values that were measured higher in the Karoo sections (Fig. 2) appear to be consistent with Smithian and Spathian age $\delta^{13}C_{carb}$ excursions in the same marine $\delta^{13}C_{carb}$ record.

The bulk sedimentary organic carbon isotope records ($\delta^{13}C_{org}$) from the Carlton Heights and Lootsberg sections provide further support for these conclusions (Fig. 2). The data also supports the magnetostratigraphic correlation of Unit II between the northern (Carlton Heights and Bethulie regions) and southern (Lootsberg and Wapadsberg regions) parts of the basin. At the Carlton Heights and Lootsberg sections, $\delta^{13}C_{org}$ decreases from ~ –24‰ Vienna Pee Dee belemnite (VPDB) to ~ –26‰ VPDB across the uppermost meter of Unit I and remains there through Unit II and into Unit III. Between 15 m and 22 m (Unit III), $\delta^{13}C_{org}$ increases in both sections to ~ –21‰ and then decreases ~1‰ at the base of Unit IV. This pattern is typical of P-T $\delta^{13}C$ records measured elsewhere in the world. The Wapadsberg and Bethulie $\delta^{13}C_{org}$ records do not show any substantial negative excursions, particularly not at the P-T boundary, but both of these sections are extensively intruded by Mesozoic dolerite dikes and sills. We suggest that this igneous activity has homogenized the primary $\delta^{13}C_{org}$ record at these two sections.

Fossil vertebrate biostratigraphy confirms that Unit II is essentially contemporaneous across the Karoo basin. At all sections, the highest occurrence of the uppermost Permian zonal index, *Dicynodon lacerticeps*, is found either immediately below (at the fossiliferous Lootsberg, Wapadsberg, and Bethulie sections) or at most several meters below the base of Unit II (at the fossil-poor Carlton Heights and Kommandodrift Dam sections). *Dicynodon lacerticeps* was never found in or above Unit II, and the first Triassic fossil common to all sections—*Lystrosaurus* sp. C—was found in the lower strata of Unit III but never in Unit II.

In summary, three independent correlation methods support our contention that Unit II is both essentially isochronous across the Karoo basin and also time equivalent with the P-T boundary in China. This allows us to use this unit as a datum surface against which our vertebrate range taxa can be plotted and to compare the patterns of extinction with those observed at other P-T sections.

Over a period of 7 years, we collected 126 skulls assigned to 21 vertebrate taxa from the sections shown here (reptile or amphibian) (Fig. 3) (*23*). We treat these taxa as species, although further study will probably result in an even greater number of taxa. We found 13 taxa in Unit I (Upper Permian), only 4 of which persist into Unit II, and 12 taxa in Units II to IV. Six of the 13 taxa

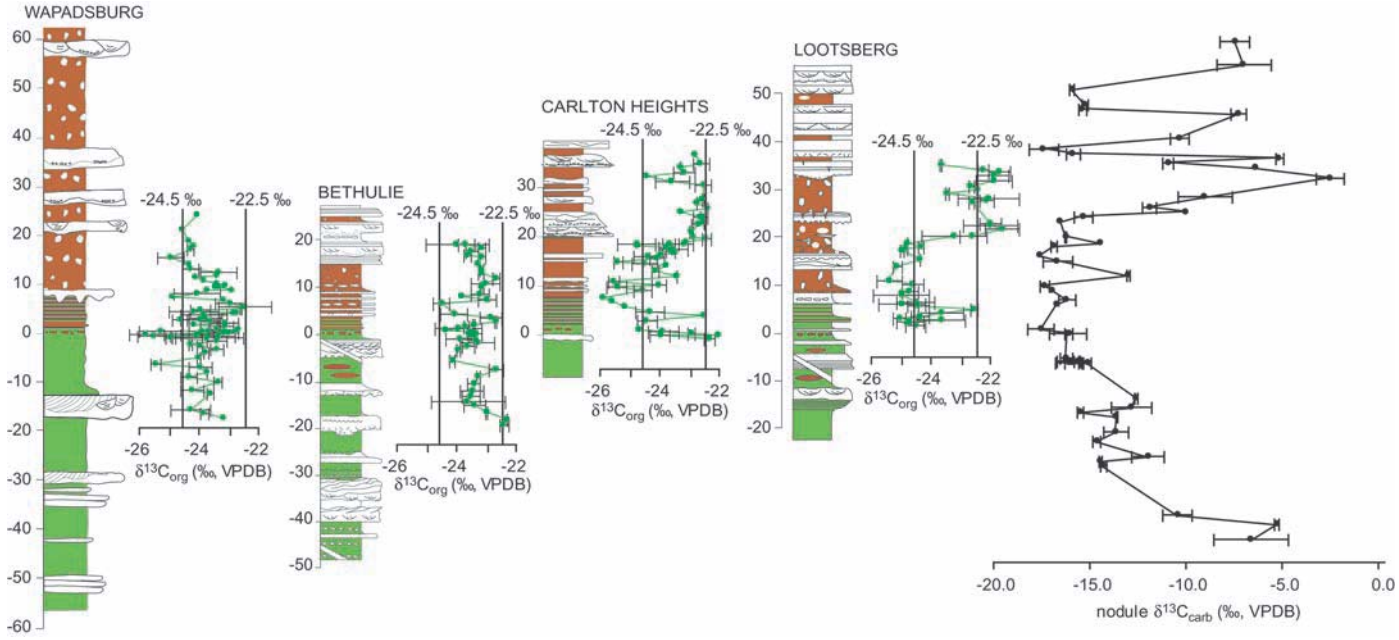

Fig. 2. The combined soil nodule $\delta^{13}C_{carb}$ record and individual lithologic and $\delta^{13}C_{org}$ records for four sections in the Karoo basin. The two sections at left (Wapadsburg, southern basin; Bethulie, northern basin) have been strongly affected by heating, as evidenced by a lack of primary paleomagnetic signal from either section. The results from Carlton Heights and Lootsberg Pass, however, have similar negative $\delta^{13}C_{org}$ excursions within Unit II, followed by an increase in $\delta^{13}C_{org}$ values in Units III and IV. The $\delta^{13}C_{carb}$ curve at the far right is combined data from carbonate nodules obtained from the Carlton Heights and the Lootsberg regions.

found in Unit I show their last appearance datums (LADs) in the last 10 m of Unit I, which suggests an enhanced rate of extinction in the latest Permian. These range terminations occurred either before or simultaneously with the reduced $\delta^{13}C_{org}$ values toward the top of Unit I.

Incomplete preservation or collection failure can make abrupt extinctions look gradual, i.e., the Signor-Lipps effect (*24*, *25*), so the assumption of simultaneous extinction of the included taxa was tested using the Kolmogorov-Smirnov (K-S) goodness-of-fit test (*26*). The case for the Karoo basin is complicated, because some of our sampled taxa (i.e., *Pristerodon* sp. and *Aelurognathus* sp.) might have become extinct before the base of Unit II or long after (*Ictidosuchoides* sp., *Thrinaxodon* sp., *Lystrosaurus* sp. C.), thereby complicating the statistical protocols (*27*). Thus, we calculated confidence intervals on stratigraphic ranges (*28*). We chose 20% confidence intervals following the improved method for testing extinction levels (*29*) for each of the nine taxa (Table 1).

Four taxa (*Theriognathus* sp., *Dicynodon lacerticeps*, *Lystrosaurus* sp. A, and *Rubidgea* sp.) appear to have become extinct at or near the base of Unit II (Fig. 3). We are also confident that *Pristerodon*, *Aelurognathus*, and the abundant and widespread taxon *Diictodon* sp. were extinct before deposition of Unit II, whereas the taxa *Lystrosaurus* sp. B, *Moschorhinus* sp., and *Owenetta* sp. became extinct during, or soon after, the initiation of sedimentation marking the Katberg Formation (Unit IV) (Fig. 3). The 90% confidence interval on the position of the mass extinction extends from 0 m (stippled level A) to about 20 m, or from the base of Unit II up into the middle part of Unit III. Thus, there is a low probability that the mass extinction of the Karoo vertebrates occurred within the Katberg Formation (stippled level B), where the mass extinction has been traditionally placed (*30*).

We have also used confidence intervals to examine the origination of taxa. Theoretically, if the majority of Permian extinctions occurred at a specific horizon, we would expect to observe, after the extinction, a follow-on origination of new species into vacated niches (or immigration into the basin). We do not observe this. By inverting the procedure for fossil disappearances, we calculated 20% range extensions downward and from this computed a 94% probability confidence interval for origination (Fig. 3). The results suggest it is probable that at least some species originated before the deposition of Unit II, whereas others originated during and after Unit II deposition. The distribution of originating taxa fails the K-S test for random distribution of new taxa at the 99% level, suggesting that Triassic taxa origination was in response to some event that occurred before the end of the Permian. We caution that new taxa origination may violate the assumption of equal probability of preservation, because new taxa are likely to be rare and uncommon. This effect may overestimate the calculated ranges for originations.

A further caveat is that we are implicitly accepting an empty-niche model brought about by the extinction, even though some or many niches may have been reconstructed

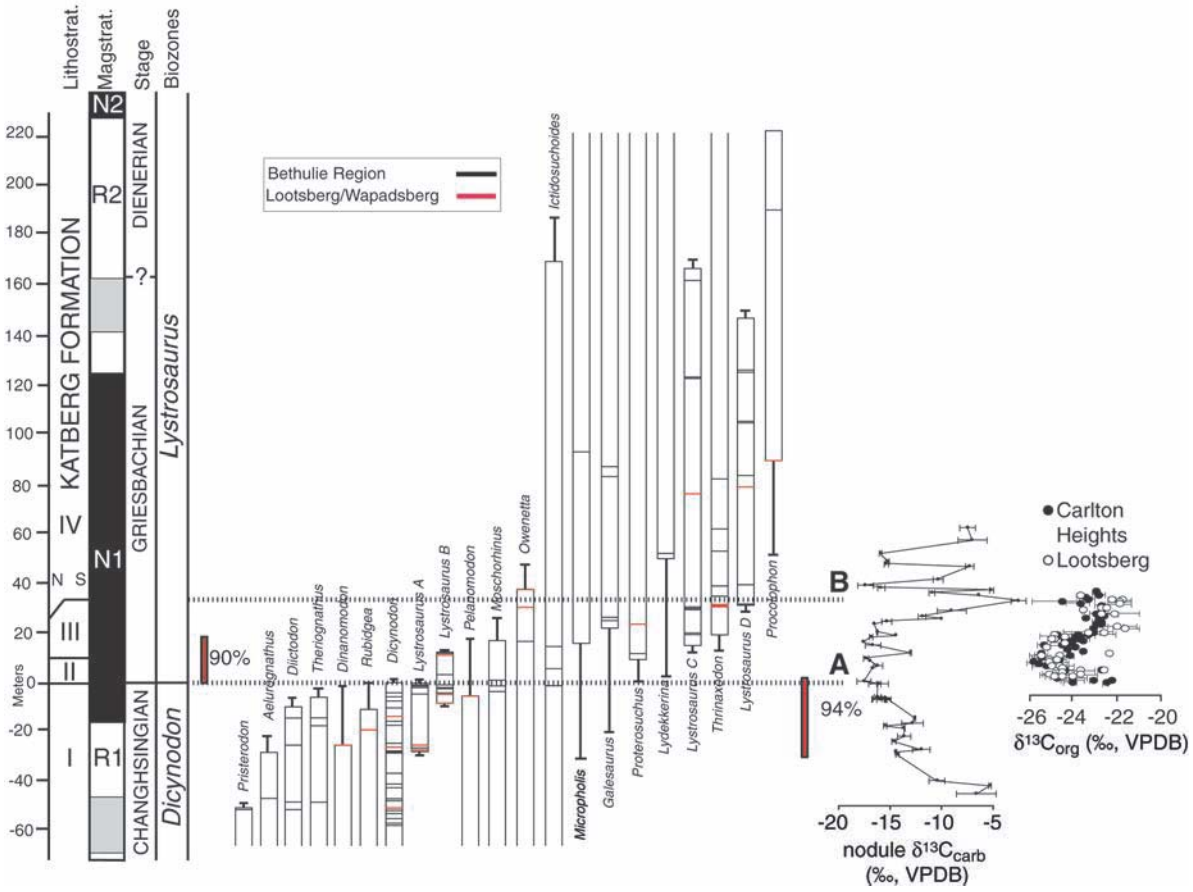

Fig. 3. Magnetostratigraphic, biostratigraphic, and carbon isotopic records from the Karoo basin. This figure can be compared with the generic range chart for the entire Permian/Lower Triassic sequence in the study area (*12*). The red bar on the left is the 90% confidence interval for Permian taxa extinction; the red bar on the right is the 94% confidence interval for Triassic taxa origination, assuming that originations were in response to catastrophic extinction. Level A is the base of Unit II, which is correlated to the highest occurrence of Permian index fossil *Dicynodon lacerticeps*. Level B is the base of Unit IV (Katberg Formation), where a spike in fungal spore abundance and the P-T boundary have been recorded previously (*32*). Of particular note is the appearance of *Lystrosaur* A and *Lystrosaur* B below the P-T boundary. *Lystrosaurs* are Triassic animals, and the appearance of two species below the P-T boundary is evidence that major evolutionary changes were under way before the end of the Permian.

and not refilled. The pattern of extinction and origination appears to be consistent with an enhanced rate of extinction coincident with or just below Unit II, but the number of extinct species there may be no more than five (eight species become extinct in Unit I). The most thorough compilation of the vertebrate record from the *Dicynodon* Zone in the Karoo (*8*) shows that 10 of 21 taxa present at the base of the ~300-m-thick zone are absent in its upper third, indicating that considerable extinction is occurring throughout the zone and not just at its top (*31*). This observation can be supported by replotting known vertebrate ranges in the Karoo such that last occurrences are sequential (*12*), based on the new data presented here and range data from lower zones (*8*). The resulting figure (fig. S4) shows what appears to be a change from an approximately constant background extinction (as recognized by the number of taxa disappearing per unit thickness of strata) below the uppermost Permian, with enhanced extinction in the *Dicynodon* Zone culminating at the P-T extinction pulse at the top of Unit I. In the Lower Triassic–aged *Lystrosaurus* Zone, there is a reduced extinction rate high in Unit II and in Unit III. Two patterns are thus apparent: gradual extinction leading up to the P-T and a pulse of even higher extinction marking the boundary. This pattern is visible both at the species level (Fig. 3) and at the generic level (fig. S4) and is also observed at Meishan among invertebrate marine fossils.

We thus suggest that factors other than the sudden extinction of taxa stimulated the origination or appearance (through emigration) of new Triassic species into the basin. Our statistical inference (and the discovery of *Lystrosaurus* sp. A and B) that Triassic vertebrate fauna may have predated the main Permian extinction pulse is unlike the pattern of mammalian radiation after the Cretaceous-Paleogene (K-P) extinction, the only clear example of a mass extinction associated with a major impact event. The pattern that we observe for the P-T is consistent with a long-term deterioration of the terrestrial ecosystem, with a heightened pulse of both extinction and origination approximately coincident with the P-T boundary.

Unfortunately, the ranges of Permian and Triassic fossil plant remains in our study sections add little information about the pattern of extinction in the Karoo basin or about the relative timing of extinction among plants and animals there. A recent palynological study at Carlton Heights (*32*) identified a spike in fungal spore abundance at the base of our Unit IV (the Katberg Formation) and claimed the fungal spike to be the top of the *Dicynodon* Zone and thus the P-T boundary. However, the study provided insufficient information to ascertain whether the base of Unit IV is Permian or Triassic in age based on palynomorphs (*33*), and we have found in all of our sections, including the site in question, that the Katburg Formation begins well above the top of the Permian.

We interpret the biostratigraphic data presented here as consistent with a period of environmental stress during the latest Permian in this basin, punctuated by a short interval of even greater perturbation, i.e., a long "press" with one (or more) pulses superimposed. A single proximal cause might explain the extinction patterns, such as long-term environmental degradation having reached a critical threshold that triggered a short-term extinction event through ecosystem collapse. Alternatively, the long- and short-term effects observed in the Karoo could have two (or more) different causes. We searched for evidence of an end-Permian bolide impact, such as the impact clays and ejecta layers found commonly in the environmentally similar Hell Creek Formation (Late Cretaceous), Montana, which are associated with the Chicxulub K-P impact. Neither our search nor previous searches in the Karoo sections for minerals associated with large-body impact (*34*) have met with success, although fluvial facies can contain hiatuses and the absence of impact evidence must be tempered with caution.

The P-T southern Karoo basin and the K-P Hell Creek Formation strata were deposited by similar fluvial systems, and they can be compared. The Hell Creek vertebrate paleontological record is constantly diverse up through the last Cretaceous zone, followed by a catastrophic extinction coeval with a negative excursion in the $\delta^{13}C$ record (*35*, *36*) and clear sedimentological and mineralogical evidence of a large-body impact; $\delta^{13}C$ returns to pre-event values within a narrow stratigraphic interval (*35*). The Karoo record is entirely different, and we conclude that if an impact occurred at all, it had a minor role in the end-Permian extinctions in the Karoo. The geologic data from the Karoo are consistent with a more protracted catastrophic ecosystem collapse than a sudden impact would produce.

Table 1. Confidence that vertebrates became extinct or originated prior to deposition of lithological Unit II by application of the equation $C = 1 - (G/R + 1)^{-(H-1)}$, where G is the interval between the highest occurrence of the taxon and the base of Unit II, R is the taxon's observed stratigraphic range, and H is the number of fossiliferous strata within the range of R (*28*). The null hypothesis of a random distribution of fossil horizons is rejected. Taxon confidence (C), extinction before deposition of Unit II. Confidence, origination before deposition of Unit II.

Taxon	Confidence (C) (extinction before deposition of Unit II)	Confidence (origination before deposition of Unit II)
Pristerodon sp.	0.875	
Aelurognathus sp.	0.5	
Diictodon sp.	0.52	
Theriognathus sp.	0.31	
Rubidgea sp.	0.2	
Dicynodon lacerticeps	0.17	
Lystrosaurus sp. *A*	0.13	
Lystrosaurus sp. *B*	0	
Pelanomodon sp.	.05	
Moschorhinus sp.	0	
Owenetta sp.	0	
Ictidosuchoides sp.	0	
Micropholis sp.		0.08
Galesaurus sp.		0.2
Proterosuchus sp.		0.25
Lydekkerina sp.		0.21
Lystrosaurus sp. C		0.69
Micropholis sp.		0.08
Thrinaxodon sp.		0.55
Procolophon sp.		0.54

References and Notes

1. D. H. Erwin, *Nature* **367**, 231 (1994).
2. A. Knoll *et al.*, *Science* **273**, 452 (1996).
3. L. Becker *et al.*, *Science* **291**, 1530 (2001).
4. A. R. Basu *et al.*, *Science* **302**, 1388 (2003).
5. L. Becker *et al.*, *Science* **304**, 1469 (2004).
6. M. J. Benton, R. J. Twitchett, *Trends Ecol. Evol.* **18**, 358 (2003).
7. Y. G. Jin *et al.*, *Science* **289**, 432 (2000).
8. B. Rubidge, *Geol. Surv. S. Afr. Biostratigraphy* **1**, (1995).
9. O. Catuneanu *et al.*, *Basin Res.* **10**, 417 (1998).
10. Two sections were sampled near Lootsberg Pass (S31, 51.005; W24, 52.299, and S31, 49.334; W24, 48.565), one section near Wapadsberg Pass (S31, 52.474; W24, 54.882), one section near Carlton Heights (S30, 35.425; W25, 439.135), one section near Kommandodrift Dam (S31, 76.506; W24, 49.980), and two sections near Bethulie (S30, 24.989; W26, 17.234, and S30, 26.675; W26, 18.006). Four lithostratigraphic facies are present: Unit I, dark gray to gray mudstones, siltstones, and sandstones with sedimentary structures typical of meandering river deposits; strata show rubification in the uppermost meters. Unit II, 3- to 5-m-thick, rhythmically bedded laminated mudrock, described as an event bed (*37*). Unit III, red concretionary mudstone and thin sandstone. Unit IV (Katberg Formation), thick olive-green sandstone with conglomeratic bases interbedded with thinner red siltsone and mudstone; sandstones have sedimentary structures typical of braided river deposits.

11. G. Retallack *et al.*, *Geol. Soc. Am. Bull.* **115**, 1133 (2003).
12. Materials and methods are available as supporting material on *Science* Online.
13. M. O. de Kock, J. L. Kirschvink, *Gond. Res.* **7**, 175 (2004).
14. All samples passed tests for baked contact, class B reversal, and magnetostratigraphic consistency. The reversal in the upper part of Lootsberg Pass was corroborated at a second parallel section ~1 km to the east, where a reversal of similar thickness was found at the same stratigraphic horizon. We have used this pattern to correlate and subdivide the Katberg Formation across the Karoo basin.
15. M. Szurlies *et al.*, *Earth Planet. Sci. Lett.* **212**, 263 (2003).
16. M. Steiner *et al.*, *J. Geophys. Res.* **94**, 7343 (1989).
17. J. Nawrocki, *Terra Nova* **16**, 139 (2004).
18. K. G. MacLeod *et al.*, *Geology* **24**, 227 (2000).
19. M. J. De Wit *et al.*, *J. Geol.* **110**, 227 (2002).
20. W. T. Holser, M. Margaritz, *Geochim. Cosmochim. Acta* **56**, 3297 (1992).
21. T. E. Cerling, *Global Biogeochem. Cycles* **6**, 307 (1992).
22. J. L. Payne, *Science* **305**, 506 (2004).
23. The actual P-T boundary is defined by the base of the Triassic system or the first appearance of the conodont *H. parvus* in marine strata. The base of the Triassic cannot be identified in the Karoo until a terrestrial index fossil is formally chosen. At present, we have placed the P-T boundary at the level of the highest Permian taxon, a practice that runs contrary to accepted stratigraphic procedure. Here, each taxon is treated as a species; we realize that taxonomic study of each is required. Pending the formal systematic treatment of *Lystrosaurus* (*38*), we designate the four separate species of *Lystrosaurus* from our study area as *Lystrosaurus* sp. A, B, C, and D.
24. P. W. Signor III, J. H. Lipps, *Geol. Soc. Am. Spec. Pap.* **190**, 291 (1982).
25. Preservational biases may also have controlled the observed pattern of extinction. However, because there are more fossils in Units III and IV than in the upper 30 m of Unit I, we would expect to find the Permian taxa if they continued higher in the section. As that is not the case, we conclude that the observed ranges are real samples of the preservable fauna in the depositional basin.
26. M. S. Springer, *Paleobiology* **16**, 512 (1990).
27. A. Solow, *Paleobiology* **29**, 181 (2003).
28. C. R. Marshall, *Paleobiology* **20**, 459 (1994).
29. S. Wang, C. R. Marshall, *Paleobiology* **30**, 5 (2004).
30. G. H. Groenwald, J. W. Kitching, *Geol. Surv. S. Afr. Biostratigraphy* **1**, 35 (1995).
31. G. M. King, *S. Afr. Mus. Sidney Haughton Mem. Lect.* **3**, 1 (1990).
32. M. B. Steiner *et al.*, *Palaeogeogr. Palaeoclimatol. Palaeoecol.* **194**, 405 (2003).
33. There has been much recent criticism of the so-called P-T fungal spike as a chronostratigraphic marker, based on the discovery of multiple horizons at some localities and the complete absence of the marker at others, most notably at the important Greenland locality (*39*), as well as the possibility that the fossils may not have come from fungi at all (*40*).
34. L. Coney *et al.*, *L.P.S.C.* **35**, 1488 (2004).
35. N. C. Arens, A. H. Jahren, *Palaios* **15**, 4 (2000).
36. P. Sheehan *et al.*, *Science* **254**, 835 (1991).
37. P. D. Ward *et al.*, *Science* **289**, 1740 (2000).
38. J. Botha, R. Smith, in preparation.
39. R. J. Twitchett *et al.*, *Geology* **29**, 351 (2001).
40. C. Foster, M. Stephenson, *First Int. Conf. Palynology, Abst.* **57** (2002).

41. We thank the NASA Astrobiology Institute, the NSF, and the National Research Foundation of South Africa for funding. Help in the field and fossil preparation came from the Karoo Paleontology Department, Iziko: South African Museum (P. October, H. Stumer, G. Farrell, preparation by A. Crean, field collection by N. Ward and T. Evans, and lab help by C. Converse and E. Steig). Paleomagnetic software used for data analysis was from C. Jones at the University of Colorado, Boulder. We thank F. Kyte and C. Looy for prereviews.

Supporting Online Material
www.sciencemag.org/cgi/content/full/1107068/DC1
Materials and Methods
Figs. S1 to S4
Tables S1 and S2
References

3 November 2004; accepted 3 January 2005
Published online 20 January 2005;
10.1126/science.1107068
Include this information when citing this paper.

Aconitase Couples Metabolic Regulation to Mitochondrial DNA Maintenance

Xin Jie Chen, Xiaowen Wang, Brett A. Kaufman,* Ronald A. Butow†

Mitochondrial DNA (mtDNA) is essential for cells to maintain respiratory competency and is inherited as a protein-DNA complex called the nucleoid. We have identified 22 mtDNA-associated proteins in yeast, among which is mitochondrial aconitase (Aco1p). We show that this Krebs-cycle enzyme is essential for mtDNA maintenance independent of its catalytic activity. Regulation of *ACO1* expression by the HAP and retrograde metabolic signaling pathways directly affects mtDNA maintenance. When constitutively expressed, Aco1p can replace the mtDNA packaging function of the high-mobility-group protein Abf2p. Thus, Aco1p may integrate metabolic signals and mtDNA maintenance.

Mitochondrial DNA (mtDNA) nucleoids have been purified from several organisms (*1*–*5*). In addition to DNA packaging proteins, which are required for mtDNA maintenance (*6*, *7*), nucleoids also contain proteins whose functions are ostensibly unrelated to mtDNA activities (*1*, *5*, *8*, *9*). We previously identified 11 proteins that are associated with mtDNA (*1*) (Table 1) and have now identified 11 more (whose gene names are indicated in bold in Table 1). These proteins can be grouped into four functional categories: (I) mtDNA transactions with no other known functions in mitochondria; (II) protein import and mitochondrial biogenesis; (III) the citric acid cycle and upstream glycolytic steps; and (IV) amino acid metabolism.

As proteins in category III could potentially connect respiratory and fermentative metabolism to mtDNA maintenance, we examined mtDNA stability in strains in which a selection of these genes were inactivated. Expression of some category III genes is repressed by glucose (*10*). Therefore, mutant cells were grown in raffinose, a fermentable carbon source that does not repress mitochondrial respiration, and then assayed for the fraction of respiratory-deficient (petite) mutants in the population. mtDNA is relatively stable in *kgd1*Δ and *kgd2*Δ cells, less so in the *pda1*Δ, *pdb1*Δ, *idh1*Δ, and *lpd1*Δ strains, and very unstable in *aco1*Δ cells (Fig. 1A). mtDNA was previously noted to be unstable when some of these genes were inactivated (*11*). Further experiments established that *ACO1* is essential for mtDNA maintenance. Southern blot analysis of total cellular DNA from nascent meiotic segregants derived from an *aco1*Δ/*ACO1* ρ^+ diploid strain showed that the *aco1*Δ spores lack mtDNA (Fig. 1B).

Aco1p, citrate synthase (CS), and two subunits of nicotinamide adenine dinucleotide (NAD^+)–dependent isocitrate dehydrogenase (collectively, the aconitase metabolon) function to produce α-ketoglutarate, a precursor to glutamate. Expression of the genes encoding these proteins is positively regulated by the glucose-repressible HAP2-5 transcription complex and the transcription factors Rtg1p and Rtg3p (*12*), which are components of the mitochondria-to-nucleus retrograde (RTG) signaling pathway (*13*). Aco1p localizes to the mitochondrial matrix, as revealed by fluorescence microscopy of an Aco1p–green fluorescent protein fusion construct (fig. S1). Like other genes in the aconitase metabolon, expression of *ACO1* becomes progressively HAP-dependent in response to increased respiratory activity when cells are shifted from glucose to raffinose medium, whereas a combined inactivation of the HAP and RTG systems leads to a 14-fold reduction of *ACO1* expression, independent of the carbon source (fig. S2).

To ask whether the HAP and RTG transcription complexes can directly affect mtDNA maintenance, we generated a diploid strain heterozygous for *hap2*Δ and *rtg1*Δ. After sporulation and dissection on rich

Department of Molecular Biology, University of Texas Southwestern Medical Center, 6000 Harry Hines Boulevard, Dallas, TX 75390–9148, USA.

*Present address: Montreal Neurological Institute, 3801 University, Montreal QC H3A 2B4, Canada.
†To whom correspondence should be addressed. E-mail: ronald.butow@utsouthwestern.edu